IOP PUBLISHING EUROPEAN JOURNAL OF PHYSICS

Eur. J. Phys. **29** (2008) 945–956 doi:10.1088/0143-0807/29/5/008

Prediction of solution properties of flexible-chain polymers: a computer simulation undergraduate experiment

José García de la Torre, José G Hernández Cifre and M Carmen López Martínez

Departamento de Química Física, Facultad de Química, Universidad de Murcia, 30071 Murcia, Spain

E-mail: jgt@um.es

Received 14 December 2007, in final form 22 April 2008
Published 29 July 2008
Online at stacks.iop.org/EJP/29/945

Abstract

This paper describes a computational exercise at undergraduate level that demonstrates the employment of Monte Carlo simulation to study the conformational statistics of flexible polymer chains, and to predict solution properties. Three simple chain models, including excluded volume interactions, have been implemented in a public-domain computer program that is the tool on which this exercise is based. The first stage considers fundamental aspects of polymer chain statistics, such as the distribution of end-to-end distance and the exponents in the power laws that relate properties to chain length, for both ideal, phantom chains and also with excluded volume effects. The numerical results are employed to predict properties of real polymer/solvent systems, such as polystyrene in cyclohexane and toluene, which are then compared to experimental data.

S This article has associated online supplementary data files

1. Introduction

Owing to their well-known importance, polymers are subjects of study in physics [1], chemistry [2], biosciences [3], material sciences [4, 5], etc. A number of functional aspects of both synthetic polymers and biological macromolecules are related to their solution properties. The properties of polymers in dilute solution are particularly important because they evidence features of the individual polymer molecules. That is why many experimental methods for polymer characterization [6] are based on their properties in dilute solution, such as the radius of gyration, diffusion coefficient or the intrinsic viscosity [7]. Then, the need for theoretical

frameworks and computational tools relating structural features and solution properties seems evident.

An essential feature of the molecular backbone of polymers is that it is flexible, due to the possibility of internal rotation around skeletal bonds. Thus, most synthetic polymers—as well as biological polymers whose secondary and higher order structure is destroyed—behave as flexible molecular chains commonly visualized as random coils. The prediction of solution properties of flexible polymers is particularly difficult because of the interplay between conformational variability and hydrodynamics. For that purpose, polymer physicists, physical chemists and biophysicists have pioneered, over the last two or three decades, an approach that is now becoming popular in other fields, namely, the computer simulation of coarse-grained models (for an overview, see [8]).

In this paper we present a computational experiment based on our public-domain computer program `POLYCARLO` that has been devised as an educational tool implementing all the above-mentioned concepts: conformational statistics and dilute solution properties, coarse-grained modelling, computer simulation (Monte Carlo) procedures, macromolecular hydrodynamics, etc. The experiment and the program have been devised with sufficient simplicity so that they can be employed in the teaching of a variety of disciplines at the undergraduate level. This paper is complemented with a supplementary document that serves as a user's guide, providing more details and results (see the last section of this paper).

2. Theory

2.1. The polymer–solvent system

The system that we consider is a dilute polymer solution, meaning that there are no interactions among different polymer chains. Many equilibrium properties of a polymer solution are experimentally accessible [5]. Here we shall concentrate on three properties that are among the most basic and commonly measured.

- *The mean square radius of gyration*, $\langle s^2 \rangle$, measures the mean size of the polymeric molecule. It can be determined by static, total-intensity light scattering.
- *The translational diffusion coefficient*, D, can be determined with various techniques, the most common of which is dynamic light scattering.
- *The intrinsic viscosity*, $[\eta]$, informs on the increase in the solvent viscosity caused by the macromolecular solute and is determined by conventional viscosimetric techniques.

The dependence of these properties on molecular weight, M, can be expressed by power-law equations (also called scaling laws [9]):

$$\langle s^2 \rangle = C_s M^{a_s}, \tag{1}$$

$$D = C_D M^{a_D}, \tag{2}$$

$$[\eta] = C_\eta M^{a_\eta}. \tag{3}$$

The most common situation for the polymer/solvent/temperature system is that corresponding to the so-called *good-solvent conditions* in which polymer–solvent interactions dominate over intramolecular polymer–polymer interactions. The solvation effect in the polymer is somehow equivalent to a repulsion between polymer segments, an effect known as excluded volume (EV). In these conditions, the power-law exponents take values $a_s \approx 1.2$, $a_D \approx -0.6$ and $a_\eta \approx 0.8$. There is a temperature (the Θ temperature) at which polymer–solvent and polymer–polymer interactions are balanced and the power-law exponents take specific values: $a_s = 1$, $a_D = -0.5$ and $a_\eta = 0.5$.

2.2. Random conformation of flexible polymer chains

Along with $\langle s^2 \rangle$, another primary indicator of the overall size and conformation of a flexible linear polymer chain is the mean square end-to-end distance, $\langle r^2 \rangle$, where $\mathbf{r}$ is the end-to-end vector of the chain. The distribution of the modulus of the end-to-end vector is characterized by a function $P(r)$, such that $P(r)\,\mathrm{d}r$ is the probability of finding a value of the modulus between r and $r + \mathrm{d}r$. Distribution functions and their moments are subjects of study in the theory of statistical mechanics of chain molecules [1, 2, 10, 11]. If the intramolecular interactions were all short-ranged (bond lengths, bond angles, etc), then $P(r)$ would be a Gaussian function. Models in which intramolecular interactions are all short-ranged neglect the long-ranged EV interactions, and therefore are only useful to represent the behaviour of polymer/solvent systems at the *theta* point. When excluded volume is introduced in the model, the theory becomes much more complicated, and a useful way to study such behaviour is computer simulation. There is a simple relationship between $\langle s^2 \rangle$ and $\langle r^2 \rangle$ for ideal flexible chains at equilibrium:

$$\langle s^2 \rangle = \langle r^2 \rangle / 6. \tag{4}$$

3. Physical models

In theoretical and computational work the polymer is represented by a chain of elements, the number of which, N, must be proportional to M. These elements are the centers where the polymer mass is located and the viscous friction with the solvent, assumed as a continuum in this coarse-grained model, takes place. The chain elements are joined by $N - 1$ connectors representing pieces of the chain or subchains.

3.1. Chain connectors

Several kinds of connectors can be used to describe the chain skeleton. Here we will consider three types.

- *Rigid links (RL).* The chain in which the only restriction is that the length of the connectors, b, is fixed, usually called *freely jointed* chain, is the most primary model for a polymer molecule.
- *Stiff springs (SS).* In this representation, the connectors are stiff springs with an equilibrium length b. The potential V_i^{spr} associated with the stretching of spring i depends on the spring length Q_i following a Hookean law,

  $$V_i^{\mathrm{spr}} = \tfrac{1}{2} H (Q_i - b)^2. \tag{5}$$

  With a high value of the constant (typically $H = 100 k_B T / b^2$), where k_B is the Boltzmann constant and T is the absolute temperature, it is assured that the fluctuation of the Q_is around the equilibrium value b is small.
- *Gaussian springs (GS).* If the subchains are sufficiently long, their end-to-end vectors $\mathbf{Q}_i$ present a Gaussian distribution, equivalent to the Boltzmann distribution corresponding to a quadratic potential. Thus, the spring potential becomes

  $$V_i^{\mathrm{spr}} = \tfrac{1}{2} (3 k_B T / b^2) Q_i^2, \tag{6}$$

  where the root-mean-squared spring length is $b = \left\langle Q_i^2 \right\rangle^{1/2}$.

If EV effects are neglected, we have the *ideal* chain model. The total potential energy of the chain would be

$$V^{\text{ideal}} = \sum_{i=1}^{N-1} V_i^{\text{spr}}. \tag{7}$$

3.2. Intrachain interactions

The ideal chain only applies to experimental systems at the *theta* state. In order to be applicable in *good solvent* conditions, the polymer model must include interactions between non-bonded elements, represented by a pair-potential V_{ij}^{EV} that will depend on the distance r_{ij} between non-connected chain elements. We consider three different descriptions of these interactions.

- *Hard-spheres interaction (HS).* In a simple representation of the EV effect, the elements are regarded as hard, impenetrable spheres of diameter d. Thus, the excluded volume potential is

$$V_{ij}^{\text{EV}} = \begin{cases} \infty & r_{ij} < d \\ 0 & r_{ij} \geqslant d. \end{cases} \tag{8}$$

  The maximum reasonable value of d should be the characteristic length of the connectors, b, but in practice smaller values, like $d = 0.5b$, are employed [13].
- *Lennard–Jones potential (LJ).* Another common representation of interaction between material particles is the Lennard–Jones potential,

$$V_{ij}^{\text{EV}} = 4\epsilon_{\text{LJ}} \left[\left(\frac{\sigma_{\text{LJ}}}{r_{ij}} \right)^{12} - \left(\frac{\sigma_{\text{LJ}}}{r_{ij}} \right)^{6} \right], \tag{9}$$

  where ϵ_{LJ} is the minimum energy and σ_{LJ} is the distance at which the potential is zero. The parameterization of this potential for polymer solutions has been described in the literature [14–16]. Within the range of parameter values able to represent good solvent conditions, we choose $\sigma_{\text{LJ}} = 0.8b$ and $\epsilon_{\text{LJ}} = 0.1k_BT$ because they reproduce quite well the scaling laws characteristic of linear flexible chains. In order to save time in the simulations, a cut-off distance, r_c, is introduced, so that for $r_{ij} > r_c$, $V_{ij}^{\text{EV}} = 0$. A proper value is $r_c = 3b$ [15, 16].
- *Soft repulsive potential (SR).* The Lennard–Jones potential has the advantage of including both attractive and repulsive interactions, but it presents the computational disadvantage that for $r_{ij} < \sigma_{\text{LJ}}$ the potential increases abruptly with decreasing r_{ij}. In order to avoid this difficulty, a repulsive potential that decays smoothly with distance has been proposed [17–19],

$$V_{ij}^{\text{EV}} = \begin{cases} A\, \mathrm{e}^{-\alpha r_{ij}} & r_{ij} < r_c \\ 0 & r_{ij} \geqslant r_c. \end{cases} \tag{10}$$

  The values of the parameters that have been reported [17, 20] are: $A = 75k_BT, \alpha = 4$ and $r_c = 0.512b$. This choice of parameters predicts correctly the scaling exponent of the polymer dimensions.

  For an excluded volume chain the total potential is

$$V^{\text{real}} = \sum_{i=1}^{N-1} V_i^{\text{spr}} + \sum_i \sum_j V_{ij}^{\text{EV}}, \tag{11}$$

where the double sum runs over all the pairs ($i \neq j$) of non-connected ($i \neq j \pm 1$) elements.

A full mechanical description of the polymer model requires the specification of both the nature of the connectors and that of the intramolecular interactions. Here, we combine the various descriptions in the following models:

- *SSSR model:* Stiff springs, soft repulsive potential.
- *GSLJ model:* Gaussian springs, Lennard–Jones potential.
- *RLHS model:* Rigid links, hard-spheres potential.

Each of these models includes the version corresponding to an ideal chain, denoted as the *SS model*, *GS model* and *RL model*.

4. Methodology

4.1. Monte Carlo procedures

The generic term 'Monte Carlo simulation' refers to a variety of simulation procedures. Here we consider two procedures, chosen according to the features of each model.

In the *SSSR* and *GSLJ* models, both the connector potential and the intramolecular potentials are continuous (except for the unimportant cutoff of the latter). The procedure employed for their simulation is a standard importance sampling procedure [21]. A Monte Carlo step begins with an initial configuration of the chain with potential energy V. For each element, a random displacement is carried out. The coordinates (x, y, z) of each bead are changed to (x', y', z'), where $x' = x + \delta x$, $y' = y + \delta y$, $z' = x + \delta z$. The displacements δx, δy and δz are random numbers with uniform distribution in the interval $(0, \Delta)$, where the maximum amplitude Δ has been adequately chosen. For the new conformation of the chain, the potential energy V' is evaluated (equation (7) for models without EV; equation (11) for models with EV). If $V' \leqslant V$, the new conformation is accepted. If $V' > V$, a random number u with uniform distribution in (0,1) is generated. If $u < \exp(-(V' - V)/k_B T)$, the new conformation is accepted; otherwise, it is rejected and the initial conformation is taken as the final one counted once again for the statistics.

In the *RLHS* model, both the connector potential and intramolecular potential are discontinuous. For this model we employ a simulation method based on the self-avoidance of the freely jointed chain during the simulation step [13]. Element i is moved within a circumference in a plane perpendicular to the line joining elements $i-1$ and $i+1$, maintaining a constant distance from them. The motion is an arc of circumference with angle ϕ (see figure 1 in [13]), which is taken as a random number with uniform distribution in the interval $(0, \Phi)$. The resulting position of the element is checked for overlapping: if the element after the step is at a distance, from any other element in the chain, smaller than d, the conformation is rejected and the previous one is counted once again. In using this procedure, initial conformation must not be a straight string of beads, otherwise this kind of move would leave the polymer chain unchanged.

There exist other more efficient Monte Carlo procedures such a reptation, pivoting or crank–shaft movements [22], widely used when performing intensive simulations on more sophisticated polymer models.

An aspect of practical importance in Monte Carlo methods is the choice of the amplitude of the Monte Carlo step, Δ or Φ. If it is too small, the probability of acceptance of the new conformation is very high, but the procedure is inefficient because the conformational space is scanned at too slow a pace. On the other hand, if the step is too large, the probability of rejection is too high, with many conformations being a copy of the previous one. The Monte Carlo step must be adjusted to give intermediate values for the rejection rate (for instance, 10–30%).

A Monte Carlo generation consists of a sufficiently large number of Monte Carlo steps. The conformations so generated are sampled with a regular interval. It is useful to decompose the sample into a certain number (five, for instance) of subsamples, and for each of them the averages are evaluated. The mean value of the subsample averages will be the final result, and their standard deviation can be considered as an estimate of the simulation uncertainty.

4.2. Calculation of properties: dimensionless quantities

For each chain conformation in the Monte Carlo sample, the three properties considered in this study are evaluated. The mean square radius of gyration is obtained as

$$\langle s^2 \rangle = \frac{1}{N} \sum_{i=1}^{N} s_i^2, \tag{12}$$

where s_i is the distance from the element i to the centre of mass, evaluated from the Cartesian coordinates.

The hydrodynamic properties D and $[\eta]$ are calculated regarding the Monte Carlo conformation as an (instantaneous) rigid body. As mentioned above, the final value for the flexible polymer will be the average over the individual values. This is the so-called *rigid-body treatment* of flexible-chain hydrodynamics [23], an upper-bound approximation [24] to the exact results, which has been shown to give accurate predictions within a few percent [17]. For these calculations, the chain elements are regarded as spherical frictional elements (beads) with radius σ and frictional coefficient $\zeta = 6\pi\eta_0\sigma$, where η_0 is the solvent viscosity. The hydrodynamic interaction between them is accounted for by means of the Rotne–Prager–Yamakawa tensor [25, 26]. The Stokes radius of the spherical beads is $\sigma = 0.257b$, corresponding to a value of the hydrodynamic interaction parameter $h^* = 0.25$ [27]. Thus, for each chain conformation, the hydrodynamic properties D and $[\eta]$ are evaluated—along with the chain dimensions—using the theory and computational procedures employed for rigid bead models. Some details about hydrodynamic tensors are included in a supplementary document, available in the online version of this paper at stacks.iop.org/EJP/29/945, and for a full description of rigid-body hydrodynamics see references [28–30].

For numerical work, it is convenient to employ reduced, dimensionless forms of the physical properties (hereafter denoted with an asterisk) which do not depend on the details of the polymer/solvent systems. The characteristic length b is used to reduce all lengths. Thus, the reduced mean square radius of gyration is given by $\langle s^2 \rangle^* = \langle s^2 \rangle / b^2$. The natural token for energy is $k_B T$. According to this, we have $D^* = (6\pi\eta_0 b / k_B T) D$ and $[\eta]^* = (M/N_A b^3)[\eta]$, where N_A is Avogadro's number.

From the power laws expressing the dependence of the physical quantities on M (equations (1)–(3)), and considering that M and the number of units in the model, N, must be proportional, it follows that the reduced quantities must follow similar scaling laws:

$$\langle s^2 \rangle^* = C_s^* N^{a_s}, \tag{13}$$

$$D^* = C_D^* N^{a_D}, \tag{14}$$

$$[\eta]^* = C_\eta^* N^{a_\eta^*}, \tag{15}$$

where the exponents a_s and a_D are the same for the reduced as for the physical quantities, while for the viscosity we now have $a_\eta^* = 1 + a_\eta$.

5. Results

The Monte Carlo simulation of the various chain models and the calculation of reduced solution properties using the rigid-body hydrodynamic treatment are implemented in a computer program, POLYCARLO. The use of this tool is remarkably simple; it requires a brief input specifying the number of chain elements, N, along with the parameters specific to each model, and some data for the Monte Carlo simulation. The output of the program consists of a set of reduced properties, $\langle s^2\rangle^*$, D^* and $[\eta]^*$, as well as $\langle r^2\rangle^*$ and the distribution $P(r^*)$ within a specified interval for r^*. The results obtained from POLYCARLO can be used in comparison with the theoretical predictions, illustrating the differences between ideal and excluded volume chains. Beyond the theoretical view, the results can also be employed to predict the values of real solution properties, both in *theta* and good solvents. This section describes the essential results and their discussion. An extensive collection of results can be found in the supplementary document available at stacks.iop.org/EJP/29/945.

5.1. Verification of theoretical results

Numerical results from POLYCARLO are reported in tables 1–6 of the supplementary document. For the conformational properties, $\langle r^2\rangle$ and $\langle s^2\rangle$, a Monte Carlo sample of 10^6 chains was generated, and 1 out of every 10 was taken for the statistics. Because calculation of the hydrodynamic properties, D and $[\eta]$, consumes much time, a Monte Carlo sample of 10^6 chains was generated in a separate run and 1 out of every 100 was taken for the statistics.

The first fundamental relationship to be tested is the chain dependence of the square end-to-end distance in ideal conditions: $\langle r^2\rangle = (N-1)b^2$ or, in reduced form, $\langle r^2\rangle^* = N-1$ (for sufficiently long chains, the number of beads, N, is practically equal to the number of connectors, $N-1$). The numerical results for the three ideal models, RL, GS and SS, confirm that this holds well within the error bar of the results (see tables 1–3 in the supplementary document). Next, the relationship between $\langle r^2\rangle$ and $\langle s^2\rangle$, equation (4), is verified. For all the models, the ratio $\langle r^2\rangle/\langle s^2\rangle$ is very close to 6, as illustrated in table 4 of the supplementary document. This happens not only for ideal chains, but also holds quite closely for EV chains [12]. Another essential aspect is the nature of the distribution of the end-to-end distance. The probability density for the reduced end-to-end distance can be written as

$$P(r^*) = \left(\frac{3}{2\pi\langle r^2\rangle^*}\right)^{3/2} 4\pi r^{*2} \exp\left[-\frac{3r^{*2}}{2\langle r^2\rangle^*}\right]. \tag{16}$$

In order to check whether $P(r^*)$ obey equation (16), the following linearization is useful:

$$\ln[P(r^*)/r^{*2}] = \ln A - Br^{*2}, \tag{17}$$

where

$$A = 4\pi\left(\frac{3}{2\pi\langle r^2\rangle^*}\right)^{3/2} \tag{18}$$

and

$$B = \frac{3}{2\langle r^2\rangle^*}, \tag{19}$$

so that

$$\langle r^2\rangle^* = \frac{3}{2\pi}\left(\frac{4\pi}{A}\right)^{2/3} \tag{20}$$

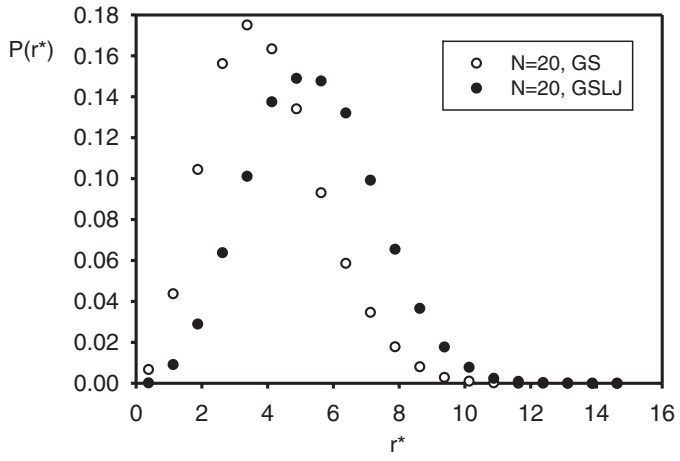

Figure 1. Histograms of the $P(r^*)$ distributions for models GS and $GSLJ$ of a chain with $N = 20$.

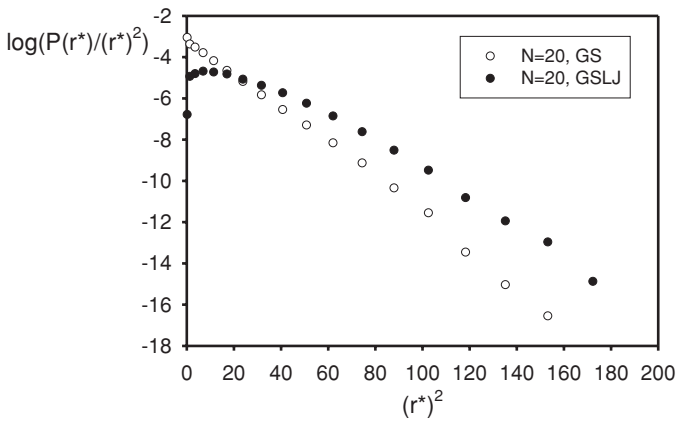

Figure 2. Plots of $\log(P(r^*)/r^{*2})$ versus r^{*2} for models GS and $GSLJ$ of a chain with $N = 20$.

or

$$\langle r^2 \rangle^* = \frac{3}{2B}, \tag{21}$$

and A and B are related through

$$A^{2/3}/B = (16/\pi)^{1/3} = 1.7204\ldots. \tag{22}$$

The aspect of the $P(r^*)$ distribution diagrams for an ideal chain and its counterpart with excluded volume is qualitatively similar. However, when the Gaussian behaviour is tested in a $\log(P(r^*)/r^{*2})$ versus r^{*2} plot, the difference becomes evident: the ideal model gives a straight line, while for the non-ideal model the trend is clearly nonlinear. Examples of this are provided in figures 1 and 2 for the GS and $GSLJ$ models of a chain with $N = 20$ beads. It is worth mentioning that the Gaussian distribution of the end-to-end distance of an ideal chain, mathematically exact in the limit of $N \to \infty$, is quite accurate even for moderately short chains. From the linear plots for the three ideal models, the least-squares fit yields the

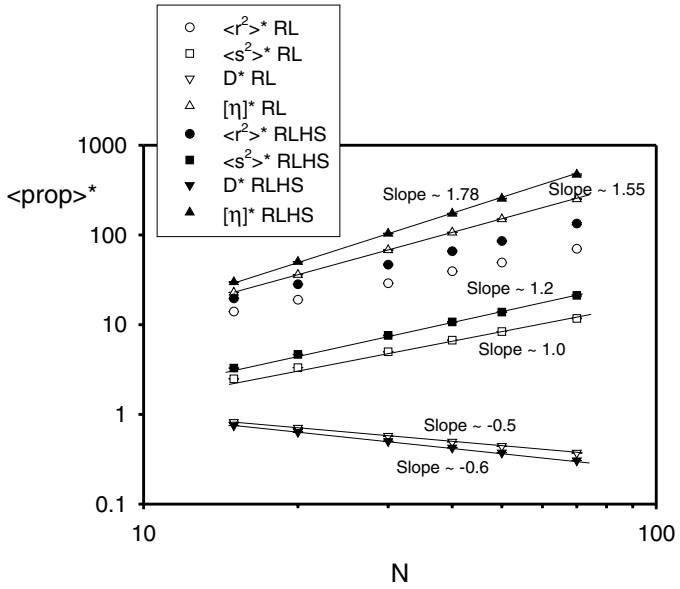

Figure 3. Log–log plots of $\langle r^2\rangle^*$, $\langle s^2\rangle^*$, D^* and $[\eta]^*$ versus N for the *RL* and *RLHS* models. The values of the slopes, corresponding to the exponents a_r, a_s, a_D and $a_{[\eta]}$, are indicated.

values of the constants A and B listed in table 5 of the supplementary document. That table also includes the values of $\langle r^2\rangle^*$ from equations (20) and (21), and the quantity defined in equation (22).

The power-law dependence of the properties $\langle r^2\rangle^*$, $\langle s^2\rangle^*$, D^* and $[\eta]^*$ on chain length is tested and analysed in log–log plots of the properties versus N (see figure 3). By least-squares fits we can obtain the C^* constants and the a exponents in equations (13)–(15). Numerical values of those constants and exponents for all the studied models can be found in table 6 of the supplementary document. The characteristic exponents for the ideal chains agree with the theoretical predictions, $a_s = 1$, $a_D = -1/2$ and $a_\eta = 1/2$ or $a_\eta^* = 3/2$. For chains with excluded volume we obtain values that are very close to the theoretical limit (corresponding to very good solvents), $a_s = 1.2$, $a_D = -0.6$ and $a_\eta = 0.8$ or $a_\eta^* = 1.8$.

5.2. Prediction of experimental properties

The numerical results from the simulation can be employed to predict values of the solution properties that can be compared with experimental data, for varying molecular weight. For that purpose, we need a minimum set of parameters that will enable us to express the dependence of the real properties on M from the simulated dependence of the reduced properties on N.

We assume that we are dealing with high-molecular-weight polymers, and accept that values for N (20, 30, 50, etc) that we have employed for the simulation are also high enough (indeed, this is confirmed by the correctly observed power-law behaviours, as in figure 3). Then, we first have to transform N values into M values. This is done by introducing a parameter,

$$M_1 = \frac{M}{N}, \tag{23}$$

Table 1. Predicted physical values of $\langle s^2\rangle$, D and $[\eta]$ for $M = 5 \times 10^5$ g mol^{-1} by using the *SS* and *SSSR* models. Comparison with experimental data.

	Polystyrene/cyclohexane/35 °C (no EV)		
Property	Experimental	*SS* model	% dev
$\langle s^2\rangle \times 10^{12}$ (cm^2)	3.95	3.86	2.3
D $\times 10^7$ (cm^2 s^{-1})	1.97	1.89	5.6
$[\eta]$ (cm^3 g^{-1})	58.69	58.79	0.2
	Polystyrene/toluene/20 °C (EV)		
Property	Experimental	*SSSR* model	% dev
$\langle s^2\rangle \times 10^{12}$ (cm^2)	9.44	7.97	15
D $\times 10^7$(cm^2 s^{-1})	1.73	1.73	0.0
$[\eta]$ (cm^3 g^{-1})	147.5	143.9	2.4

which can be interpreted as the molecular weight assigned to a bead in the model. Thus, the number of beads corresponding to a certain molecular weight is $N = M/M_1$. On the basis that the value of N corresponding to the smallest polymer is sufficiently high, the results will not depend on the choice of M_1.

The other parameter that we have to specify is the physical value for the root-mean-squared spring length, b. For this assignment, it is particularly useful in the employment of the experimental radius of gyration. Considering equations (13) and (23), and that $\langle s^2\rangle^* = \langle s^2\rangle/b^2$, it turns out that

$$b^2 = \frac{\langle s^2\rangle}{\langle s^2\rangle^*} = \frac{\langle s^2\rangle}{C_s^*(M/M_1)^{a_s}}. \tag{24}$$

Thus, after the (reasonable but arbitrary) choice of M_1, having just one experimental value of $\langle s^2\rangle$ for a sample of known M, and employing the values of C_s^* and a_s of the model being considered, then the value of b can be inferred from equation (24).

Having the model parameterized (M_1 assigned and b determined) in this way, values of experimental properties can be predicted for any molecular weight by transforming into physical forms the values of the quantities that can be computed from the reduced forms:

$$\langle s^2\rangle = b^2\langle s^2\rangle^* = b^2 C_s^*(M/M_1)^{a_s}, \tag{25}$$

$$D = \frac{k_B T}{6\pi\eta_0 b} D^* = \frac{k_B T C_D^*(M/M_1)^{a_D}}{6\pi\eta_0 b}, \tag{26}$$

where η_0 is the solvent viscosity and $k_B T$ is the Boltzmann factor,

$$[\eta] = \frac{N_A b^3}{M}[\eta]^* = N_A b^3 C_\eta^*(M/M_1)^{a_\eta^*} M^{-1}. \tag{27}$$

It should be recalled that the parameters are model-dependent, and also specific to each polymer/solvent/temperature system.

Experimental power-law relationships can be found in polymer handbooks. In this way, property values for a real polymer/solvent/temperature system can be computed easily and compared to the values predicted with the above methodology. For example, in order to test *theta* solvent conditions, we suggest modelling the well-known system polystyrene in cyclohexane at 35 °C ($\eta_0 = 0.768$ cP). In [31], we find for that system, $\langle s^2\rangle = 7.90 \times 10^{-18} M$ cm^2, $D = 1.39 \times 10^{-4} M^{-0.5}$ cm^2 s^{-1} and $[\eta] = 0.083 M^{0.5}$ cm^3 g^{-1}. On the other

hand, in order to test good solvent conditions, we suggest the system polystyrene in toluene at 20 °C ($\eta_0 = 0.587$ cP), for which $\langle s^2 \rangle = 1.56 \times 10^{-18} M^{1.19}$ cm^2, $D = 3.40 \times 10^{-4} M^{-0.578}$ cm^2 s^{-1} and $[\eta] = 0.0102 M^{0.73}$ cm^3 g^{-1}.

Table 1 presents a comparison of the predictions made with the *SS* and *SSSR* models with the experimental values for a sample with $M = 5 \times 10^5$ g mol^{-1}. In table 8 of the supplementary document we compare the calculated and experimental values for all the models and two molecular weights. The typical error of the predictions between calculated and experimental values (rms percent difference) is about 5% only. In spite of the simplicity of the models and computational procedures, their predictive capability is thus well demonstrated.

6. Computer program and supplementary material

The `POLYCARLO` computer program, executable in several Windows and Linux platforms, along with a supplementary document (User Guide) containing the required information to run the program, examples of results and further details, as well as an example of input file are freely available from our website http://leonardo.inf.um.es/macromol, where other related computer programs can be found.

Acknowledgments

This work has been supported by grant 04531/GERM/06 (*Grupos de Excelencia, Región de Murcia*) and grant CTQ2006-06381/BQU from *Ministerio de Educación y Ciencia* including FEDER funds. JGHC is the recipient of a *Ramón y Cajal* postdoctoral research contract.

References

[1] Rubinstein M and Colby R H 2003 *Polymer Physics* (New York: Oxford University Press)
[2] Sun S F 2004 *Physical Chemistry of Macromolecules* 2nd edn (New Jersey: Wiley)
[3] van Holde K E, Johnson W C and Shing Ho P 1998 *Physical Biochemistry* (Englewood Cliffs, NJ: Prentice-Hall)
[4] Cowie J W G 1991 *Polymers: Chemistry and Physics of Modern Materials* 2nd edn (Boca Raton, FL: CRC)
[5] Munk P and Aminabhavi T M 2002 *Introduction to Macromolecular Science* 2nd edn (New York: Wiley)
[6] Tanaka T (ed) 2000 *Experimental Methods in Polymer Science* (San Diego: Academic)
[7] Teraoka I 2002 *Polymer Solutions* (New York: Wiley)
[8] Kröger M 2005 *Models for Polymeric and Anisotropic Liquids* (Heidelberg: Springer)
[9] De Gennes P G 1979 *Scaling Concepts in Polymer Physics* (Ithaca, NY: Cornell University Press)
[10] Flory P J 1969 *Statistical Mechanics of Chain Molecules* 1st edn (New York: Wiley)
[11] Yamakawa H 1971 *Modern Theory of Polymer Solutions* (New York: Harper and Row)
[12] Kumar K S and Prakash J R 2003 *Macromolecules* **36** 7842–56
[13] Baumgartner A and Binder K 1979 *J. Chem. Phys.* **71** 2541–5
[14] Freire J J, Rey A and García de la Torre J 1986 *Macromolecules* **19** 457–62
[15] Rey A, Freire J J and García de la Torre J 1987 *Macromolecules* **20** 342–6
[16] Rey A, Freire J J and García de la Torre J 1987 *Macromolecules* **20** 2386–90
[17] Rey A, Freire J J and García de la Torre J 1992 *Polymer* **33** 3477–82
[18] López Cascales J J and García de la Torre J 1991 *Polymer* **32** 3359–63
[19] Knudsen K D, Elgsaeter A and García de la Torre J 1996 *Polymer* **37** 1317–22
[20] Freire J J and Rey A 1990 *Comput. Phys. Commun.* **61** 297–303
[21] Newman M E J and Barkema G T 1999 *Monte Carlo Methods in Statistical Physics* (Oxford: Clarendon)
[22] Binder K (ed) 1995 *Monte Carlo and Molecular Dynamics Simulations in Polymer Science* (New York: Oxford University Press)
[23] Zimm B H 1980 *Macromolecules* **13** 592–602
[24] Fixman M 1983 *J. Chem. Phys.* **78** 1588–93
[25] Rotne J and Prager S 1969 *J. Chem. Phys.* **50** 4831–7
[26] Yamakawa H 1970 *J. Chem. Phys.* **53** 436–43
[27] Öttinger H C 1987 *J. Chem. Phys.* **86** 3731–49
[28] Harvey S H and García de la Torre J 1980 *Macromolecules* **13** 960–4

[29] García de la Torre J, Navarro S, López Martínez M C, Díaz F G and López Cascales J J 1994 *Biophys. J.* **67** 530–1
[30] García de la Torre J, del Río Echenique G and Ortega A 2007 *J. Phys. Chem.* B **111** 955–61
[31] Kurata M and Tsunashima Y 1989 Viscosity–molecular weight relationships and unperturbed dimensions of linear chain molecules *Polymer Handbook* 3rd edn ed J Brandrup and E H Immergut (New York: Wiley) p VII/1 ff